PHYSICAL REVIEW B **67**, 165307 (2003)

# Physics of imaging *p-n* junctions by scanning tunneling microscopy and spectroscopy

N. D. Jäger,[1] M. Marso,[2] M. Salmeron,[3] E. R. Weber,[3,4] K. Urban,[1] and Ph. Ebert[1,*]
[1]*Institut für Festkörperforschung, Forschungszentrum Jülich GmbH, 52425 Jülich, Germany*
[2]*Institut für Schichten und Grenzflächen, Forschungszentrum Jülich GmbH, 52425 Jülich, Germany*
[3]*Materials Sciences Division, Lawrence Berkeley National Laboratory, Berkeley, California 94720*
[4]*Department of Materials Science, University of California, Berkeley, California 94720*

(Received 24 June 2002; published 10 April 2003)

Combined voltage-dependent scanning tunneling microscopy (STM) images with atomic resolution, local scanning tunneling spectroscopy, and simulations of the potential distribution in the interface-STM tip system are used to extract the physical imaging mechanisms of GaAs *p-n* interfaces in STM images. It is shown that (i) the tip-induced changes of the potential near the interface result in the tunneling characteristics of the *p*-type (*n*-type) layer being dragged into the interfaces' depletion region at positive (negative) sample voltage. (ii) This leads to a considerable reduction of the apparent width of the image of the depletion zone in STM images. (iii) At small negative sample voltages, a pronounced depression line appears. The depression is directly correlated with the electronic interface. It arises from the interplay of competing current contributions from the valence and conduction bands. This understanding of the imaging process allows us to develop methods on how to extract accurate physical data about the properties of the electronic interfaces from scanning tunneling microscopy images.

DOI: 10.1103/PhysRevB.67.165307 PACS number(s): 73.61.Ey, 68.37.Ef

## I. INTRODUCTION

The performance of semiconductor devices is to a large degree governed by build-in band discontinuities and electrostatic potentials. The smaller the devices get, the more accurate measurements of these potential variations at interfaces need to be. Of particular interest are their spatial position, strength, and extension. Scanning tunneling microscopy (STM) has proven to be a very successful tool for the characterization of interfaces in semiconductor multilayer structures. These investigations are done mostly on cleavage surfaces in a cross-sectional geometry, where the tip images the different layers on a surface perpendicular to the growth direction.[1] This technique made it possible to image and identify, e.g., *p-n* junctions in Si and III-V semiconductors.[2–9] Although quantitative measurements of potential variations crucially require a physical understanding of the imaging process of *p-n* interfaces, this task turned out to be very difficult. First, the contrast of *p*- and *n*-doped layers varies considerably between different reported measurements even under identical tunneling conditions.[8,10] Second, many measurements were performed on Si surfaces[2–4] or on passivated surfaces.[5,6] Silicon surfaces have, however, pronounced bands of surface states in the band gap, which pin the Fermi energy position and dominate the contrast of the STM images, such that it becomes difficult to characterize the underlying *p-n* interfaces. Passivating Si or III-V semiconductor surfaces is a very complicated task although well established. In particular the electronic properties are difficult to obtain reproducibly and so far no atomic resolution has been obtained for any interface on passivated surfaces. In addition the passivation technique can etch the surfaces, such that an additional topographic contrast is introduced,[3] which makes the extraction of the interface contrast significantly more difficult. In view of this situation, we concentrated on GaAs surfaces obtained by cleavage in ultrahigh vacuum. Such surfaces are free of surface states, very reproducible, and allow imaging of *p-n* interfaces by STM with atomic resolution.[8,9,11]

In this paper, we address the physical imaging mechanisms of GaAs *p-n* interfaces by measuring voltage dependent STM images with atomic resolution combined with scanning tunneling spectroscopy. These measurements and complementary simulations of the potential of the interface-STM tip system allow us to conclude that: (i) the changes the potential distribution near the interface induced by the tip[6,12,13] shifts the tunneling characteristics of the *p*-type (*n*-type) layer into the interfaces' depletion region at positive (negative) sample voltage. Consequently, the transition region in the STM image does not coincide with the true depletion region and the apparent width of the image of the depletion zone in STM images is reduced considerably. (ii) At small negative sample voltages, a pronounced depression line appears. The depression is directly correlated with the electronic interface. It arises from the interplay of competing current contributions from the valence band and the conduction band.

Taking these physical imaging mechanisms into account we show that (i) the location of the electronic interface itself, i.e., the plane where the Fermi energy crosses the midgap position and (ii) the *real bulk* width of the depletion zone can be extracted accurately from STM images, although the *apparent* width of the depletion zone in the STM images is always too small.

## II. EXPERIMENT

We investigated a model structure consisting of molecular beam epitaxy grown *p-n* GaAs(001) multilayers. Each layer had a nominal thickness of 30 nm. The *p*- and *n*-doped layers had carbon and silicon concentrations of $(5\pm1)\times10^{18}$ and $(4\pm1)\times10^{18}$ $\mathrm{cm}^{-3}$, respectively. We cleaved these samples in ultrahigh vacuum ($1\times10^{-8}$ Pa) along a {110} plane exposing a cross-sectional view of the multilayer structure on the cleavage surface. Without breaking the vacuum, these cross sections were directly imaged by scanning tunneling microscopy.

During scanning of constant current STM images, we acquired current-voltage tunneling spectra of the differently doped layers. The spectra were measured by interrupting the feedback loop locally, keeping the tip-sample separation unchanged during the voltage sweep. The tip-sample separation itself was determined by a set point of $-2.5$ V voltage applied to the sample and 100 pA tunneling current. However, at different spatial positions even identical set points do not necessarily yield identical tip-sample separations, because the current is primarily determined by the local electronic structure of our $p$-$n$ multilayers. Thus even on atomically flat surfaces, if the underlying surface exhibits local variations in the electronic structure, the tip height changes. In order to allow a direct comparison of the different spectra we corrected all curves to identical tip-sample separation by measuring at a voltage of $-2.5$ V the exponential dependence of the current $I$ as a function of tip-sample distance $z$, $I=I_0e^{-2\kappa z}$ right before spectroscopy acquisition. In addition, each shown spectrum is an average of several spectra in order to improve the signal to noise ratio.

## III. RESULTS

Figure 1(a) shows a cross-sectional STM overview of several $p$- and $n$-doped layers. The $p$- and $n$-doped layers are separated by lines with a darker contrast, whereas the doped layers themselves have both a brighter contrast. The individual bright hillocks with a diameter of about 3 to 5 nm are signatures of negatively charged $C_{As}$ and positively charged $Si_{Ga}$ dopant atoms in the first several layers.[11,14] Under the particular tunneling conditions used, the contrast of the $p$-doped layers is slightly brighter than the contrast of the $n$-doped layers. We identified the $n$- and $p$-doped layers on basis of the growth sequence, secondary ion mass spectra, and tunneling spectra. In Fig. 1(b) an atomically resolved image of a $p$-$n$ junction recorded at $-2.0$ V is shown. The corrugation maxima, which are marked by black dots, are spaced 0.4 and 0.56 nm in $[1\bar{1}0]$ and $[001]$ direction, respectively, i.e., the size of the unit cell. A shift in the registry of the maxima is apparent. The maxima on the $n$-type side are shifted relative to those on the $p$-type side by half a unit cell in $[1\bar{1}0]$ direction. Note that the surface is atomically flat. All contrast in Fig. 1 is purely based on electronic effects.

Figure 2 shows tunneling spectra obtained in the $p$- and $n$-doped layers as well as above the lines with a darker contrast (depression line). These spectra were normalized to same tip-sample separation as described above, such that they are directly comparable. The spectra with filled triangle (▲) and circles (●) exhibit a shift of about 1 eV, which is a typical $p$- and $n$-type characteristic based on the different Fermi level positions, respectively.[8] The spectrum taken above the depression line (□) has an apparently widened band gap typical for a depletion zone.[8] A particular feature is that spectra obtained above the depletion zone have nearly

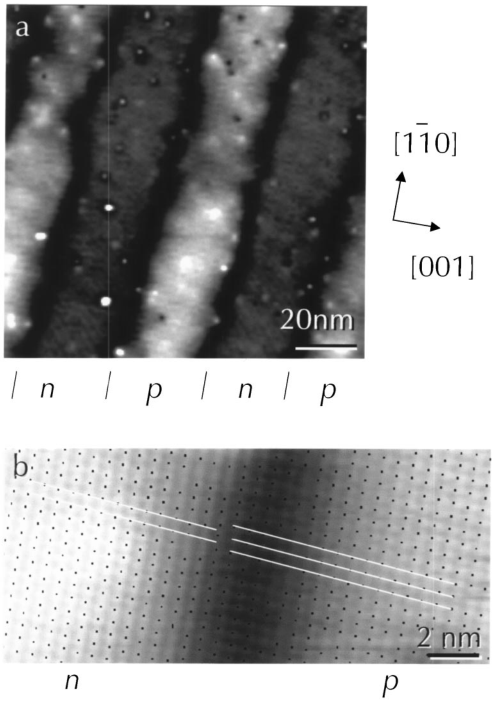

FIG. 1. Constant-current scanning tunneling microscopy images of multiple $p$- and $n$-doped layers recorded at $-2$ V sample voltage and 0.1 nA current. (a) Large scale overview: The $p$-type layers appear slightly brighter compared to the $n$-type layers. At the interfaces a pronounced depression line is observed. Bright hillocks are signatures of dopant atoms. (b) Atomically resolved image: The black dots mark the positions of the corrugation maxima. A clear shift can be seen between the maxima on the $n$- and $p$-doped sides. The white lines should guide the eye.

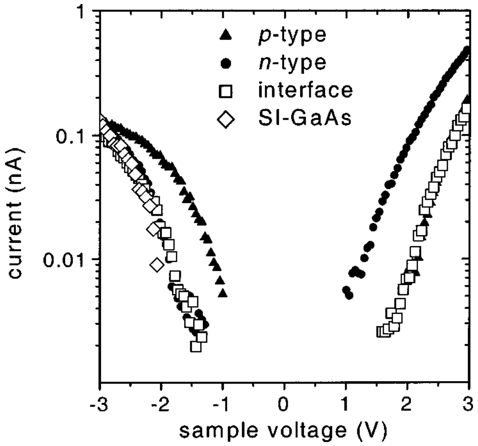

FIG. 2. Scanning tunneling current-voltage curves recorded on the $p$-type layer (▲), $n$-type layer (●), and at the interface (□) between the layers (depression line of Fig. 1). These spectra are corrected to a constant tip-sample distance for adequate evaluation (see text). For comparison a curve obtained on semi-insulating GaAs (◇) is included.

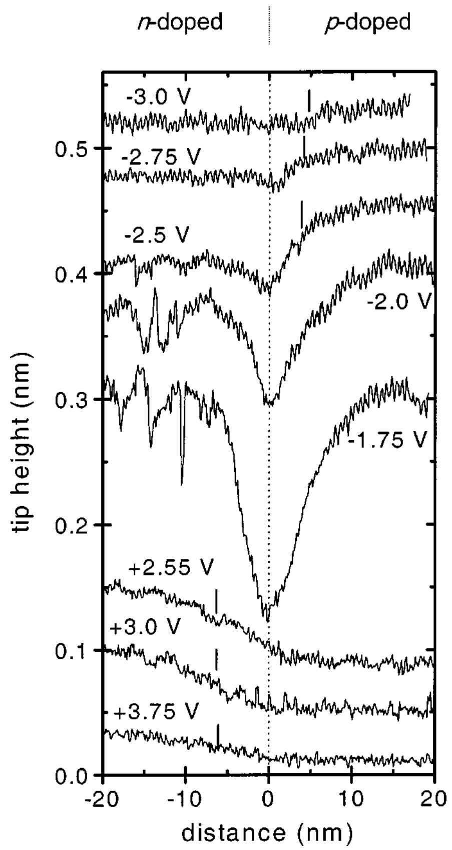

FIG. 3. Tip height in constant current STM images across a $p$-$n$ junction at various sample voltages. The small continuous wiggles arise from the atomically resolved lattice. Narrow sudden elevations and depressions are due to dopant atoms near the surface. The profiles are aligned, but are offset along the tip height axis for display. For negative sample voltages the apparent STM topography change occurs on the *p*-doped side of the junction, whereas for positive sample voltages it occurs on the *n*-doped side of the junction. For small negative sample voltage a pronounced depression is seen at the interface.

exactly the same values for negative (positive) voltage as spectra obtained on *n*- ($p$-) doped layers. For comparison we also show a tunneling spectrum on semi-insulating GaAs(110) surfaces (◇ symbols in Fig. 2).[15] The spectrum exhibits only currents at negative voltages, which are nearly identical to those obtained on the *n*-doped layer and on the depletion zone.

The dark depression line separating the *p*- and *n*-doped areas found in Fig. 1 is strongly voltage dependent and only appears in a limited voltage range. Figure 3 shows a series of height profiles over a $p$-$n$ junction taken from images measured at different voltages ranging from $-3.0$ to $+3.75$ V. The small height modulation with a periodicity of 0.56 nm is due to the atomic resolution of the atomic rows. The somewhat stronger atomically localized height changes are the signatures of point defects, which are not of interest here. In the following description we only focus on the height changes in the nm range. The pronounced depression is only visible for small negative voltages. The depth and width of this depression decreases with increasing negative tunneling voltage, whereas no depression is found at positive voltages. At negative voltages the height (contrast) is higher on the *p*-doped than on the *n*-doped layer. At positive voltage the opposite contrast occurs. The transition from low to high occurs for negative sample bias within the *p*-doped layer and for positive sample bias within the *n*-doped layer (see dashes in Fig. 3). With increasing negative or positive voltage the contrast between the differently doped layers decreases continuously. At high magnitudes of voltages nearly no contrast remains. Note at positive voltages the transition between the two differently doped layers is monotonic.

## IV. DISCUSSION

In a simple picture the contrast of the $p$-$n$ junction in the STM images is the signature of the potential changes across the junction. The potential difference (times the elemental charge) between adjacent *p*-type and *n*-type layers is the difference in the respective Fermi energy positions relative to the band edges. For highly doped *n*-type and *p*-type material, the Fermi level is close to the conduction band edge and the valence band edge, respectively. Therefore, the potential difference times the elemental charge is approximately the bandgap energy, i.e., about 1.4 eV. Thus at negative sample voltage, with no tip-induced band bending the number of occupied states between the valence band edge and the Fermi level of the tip is higher on the *p*-doped than on the *n*-doped layer *and* this number increases monotonically as one goes from the *n*-type to the *p*-type layer over the depletion zone. One should therefore expect that the tunneling current composed of carriers tunneling out of all filled semiconductor states that fall between the tip and sample Fermi level should increase monotonically from the *n*- to the *p*-doped layer. For positive voltages, where the electrons tunnel into the empty conduction band states, one should expect in analogy that the current increases from the *p*- to the *n*-doped layer, again monotonically. Thus, if the contrast of STM images of $p$-$n$ junctions was exclusively based on the potential difference between *n*- and *p*-type materials, one should only measure monotonic changes in current while crossing the interface. The location of the changes should be directly correlated to the position of the depletion zone, and their width should be that of the depletion zone, i.e., about 30 nm in our case, and essentially equally distributed on the *p*- and *n*-doped layer. This is, however, not the case. Several features are inconsistent with that simple picture. (i) The observation of the depression. (ii) For negative sample voltage ($V<-2.5$ V) the tip height changes only within the *p*-type layer and not over the entire depletion zone. (iii) At positive sample voltages the contrast change takes place over a distance of about 15 nm only in the *n*-type layer. (iv) The width of the apparent depletion zone in STM images is much smaller than that of the real depletion zone.

In the following we will first discuss the spectroscopy (current-voltage and height profiles), second extract experimentally the physical effects involved in the STM imaging, then provide a simulation of the STM-tip–$p$-$n$-junction system, and finally discuss how to extract quantitatively properties of the $p$-$n$ junction from STM measurements.

### A. Current-voltage spectroscopy

As mentioned above, the current-voltage spectra taken on the *n* layer, *p* layer, and dark depression lines are typical for *n*-type, *p*-type, and the depletion zone, respectively.[8] The spectrum obtained above the dark lines (□) is having nearly exactly the same values for negative (positive) voltage as the spectrum obtained on *n*- (*p*-) doped layers. In comparison the tunneling spectrum on semi-insulating GaAs(110) [◇ symbols in Fig. 2] matches quite well the curves of the dark lines (and the *n*-type layer) at negative sample voltage, while conversely at positive voltage no current can be obtained. From this one can deduce that the position of the Fermi energy is not the (only) determining factor of the spectra, because the Fermi energy is in the middle of the band gap for the spectrum taken in the center of the depletion zone as well as that taken on semi-insulating GaAs. Therefore, the tip-induced band bending[6,9,16] needs to be considered and obviously the degree of band bending at the semiconductor surfaces must be different in the depletion zone compared to the semi-insulating material. Because at positive sample voltages tunnel current can be found for tip locations in the depletion zone, the tip induced band bending must be smaller in the depletion zone of our *p*-*n* junction compared to semi-insulating GaAs. While the Fermi energy is in both cases equal, the surroundings are different: In semi-insulating GaAs the Fermi level is globally near midgap, while the depletion zone is sandwiched between the *n*- and *p*-type neighborhoods. The fact that the spectrum taken at the depression zone matches that of the *n*-type material for negative bias implies that the effective valence and conduction band edge positions are comparable in the *n*-type layer and the depletion zone at negative voltages. Likewise for positive bias, the tip-modified band edge positions on the depletion zone must be equal to that found in *p*-type material. This suggests that the tip-induced band bending drags the *n*-type potential from the *n*-type layer into the interfaces' depletion zone at negative voltages.[12,13] In analogy, the tip-induced band bending drags the *p*-type potential from the *p*-type layer into the interfaces' depletion zone at positive voltages.

### B. Voltage dependence of height profiles

As the tip is scanned from the *n*-type to the *p*-type material with negative sample voltage in the range of $-2.5$ to $-3$ V, the tip height does not change while the tip is above nominally *n*-doped material. Once the tip crosses from the nominally *n*-doped into the *p*-doped layer, the height of the tip increases over a distance of 10 to 15 nm. Assuming that most of the tunneling current is carried by states near the tip of the valence band, we can conclude from our experimental observations that the energetic position of the valence band edge at the tip location remains constant for any tip position within the *n*-type material and changes only in the *p*-type layer.

In contrast for positive sample voltages the tip height remains constant in the nominally *p*-doped layer and all height changes are limited to the *n*-doped layer within 10 to 15 nm from the interface. Thus, for a given positive sample voltage the energetic position of the conduction band edge at the tip position must be constant in the whole *p*-doped layer and changes only in the *n*-doped layer.

The height profiles and the conclusions drawn from them match our above discussion of the current-voltage spectroscopy data that shows that for negative sample bias the current at the interface is similar to the current found in the *n*-type layer far from the interface, while for positive sample voltage the current is similar to the current found in the *p*-type layer far from the interface. This is another indication of the importance of the tip-induced band bending[6,9,16] in the imaging of the interface region.

In this context we note that we directly observe that our surfaces have a very low concentration of defects, such as vacancies or steps, that could pin the Fermi level.[17] In addition, the tip is separated from the sample by approximately 0.5 to 2 nm. At such large separations the charge density of metal-induced gap states is very low.[18–20] Thus our surfaces are unpinned. That is, without a tip, the Fermi energy and the band edges at the surface equal those in the bulk. Therefore, we concentrate in the following on the interplay of the tip-induced band banding and the build-in potential,[12,13] to explain the contrast in the STM images and determine a method to extract interface properties from the STM measurements.

### C. Simulation of the potential in a *p*-*n*-junction–STM tip system

In order to discern the effect of the band bending induced by a metal tip located at a *p*-*n* junction and the build-in potential, we employed the two-dimensional device simulator ALTAS (version 4.3.0.R) by SILVACO international.[21] This simulator solves the two-dimensional Poisson equation yielding the potential at each location of our model device, which consists of a *p*- and *n*-doped region and a flat gate, which mimics the tip. The model device is chosen to span 100 by 100 nm. The gate is chosen to be 4 nm wide, corresponding to a tip radius on the order of 2 nm. The gate was placed 1 nm above the semiconductor surface, which is a typical tip-sample separation. Ideal contacts are put to the *n*- and *p*-type areas and those contacts have the same potential. The *n*- and *p*-type areas were modeled with dopant concentrations of $3\times10^{18}$ and $4\times10^{18}$ cm$^{-3}$, respectively. The resulting potential distribution is shown as overlying contour and gray-scale plots in Fig. 4 for various positions of the gate relative to the interface and for sample voltages of $-3$ and $+3$ V. The gate position is indicated by the small triangle. From this data we extract the potential underneath the tip, in the following called ''surface potential.'' Figure 5 shows the corresponding energetic positions of the valence and conduction band edges underneath the center of our modeled tip as a function of tip position. The values underneath the left and right end of the modeled tip follow the same qualitative behavior.

Figure 4 demonstrates clearly that the tip deforms strongly the potential distribution, especially directly underneath the tip position in an area of about 30 nm in diameter in agreement with a previous simulation.[13] For positive sample voltages the potential underneath the tip is pulled

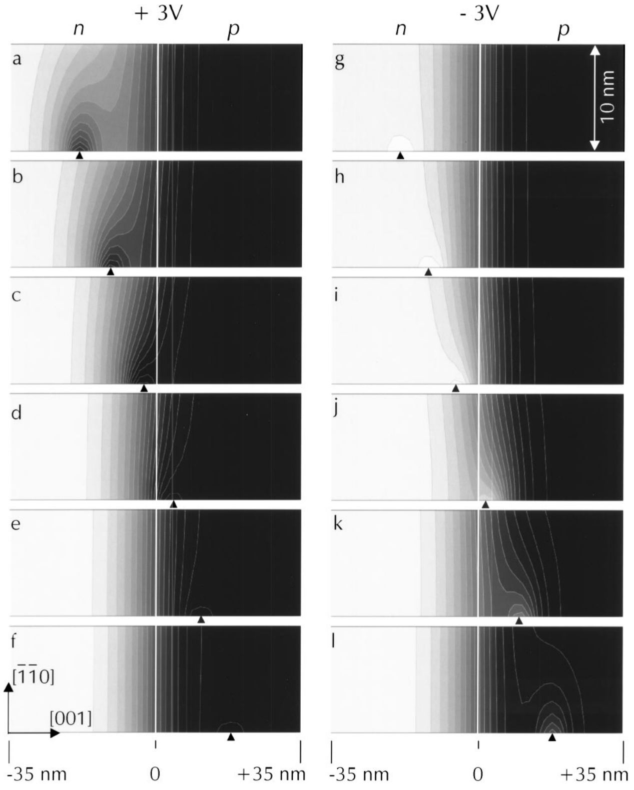

FIG. 4. Contour plots of the modeled potential distribution of a *p*-*n* junction in the presence of a biased gate at various positions indicated by the black triangle. The metallic gate is chosen to be 4 nm wide and separated 1 nm from the semiconductor, mimicking a typical STM tip geometry. The calculation was performed for a 100 nm×100 nm big slap of semiconductor material, contacted at the outer end of the *p*- and *n*-doped areas. These contacts are at +3 V for plots (a)–(f), and at −3 V for plots (g)–(l) relative to the gate. The gray scale range is from 0 (black) to 1.7 V (white).

downward. For negative sample voltages the potential underneath the tip is pulled upward. Several asymmetries are apparent: (i) For negative voltages the influence of the tip is weaker on the *n*-doped than on the *p*-doped area [compare Figs. 4(g) and 4(l)]. For positive values the situation is reversed [compare Figs. 4(a) and 4(f)]. This can be seen quantitatively in Fig. 5. (ii) The presence of a tip near the interface "pushes" the equipotential lines in the direction of the *n*-doped side for positive voltage [Figs. 4(c) and 4(d)] and towards the *p*-doped side for negative voltage [Fig. 4(i)]. Accordingly for negative voltages the potential underneath the tip for various tip positions does not change significantly for tip positions on the *n*-doped side. It only changes in the *p*-doped area [see Fig. 5(b)]. For positive values the situation is again reversed, i.e., all change of the surface potential occurs in the *n*-doped area only. As a consequence the lateral extend of the change from *p*- to *n*-type surface potential is much smaller than the width of the bulk depletion zone (compare dashed lines with symbols in Fig. 5).

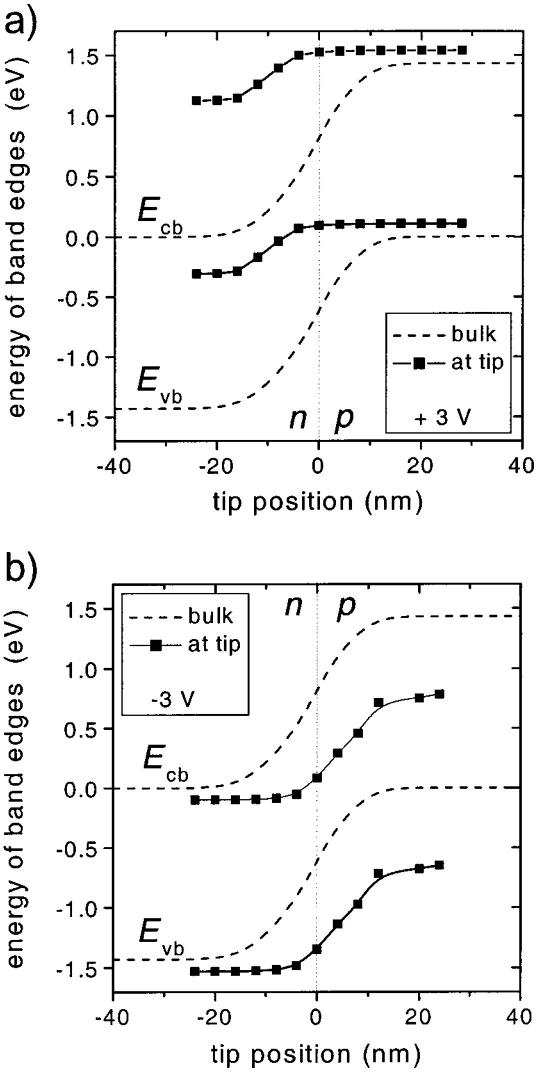

FIG. 5. Energetic positions of the conduction and valence band edges underneath the tip as a function of tip position of our model *p*-*n*-junction–STM-tip device extracted from Fig. 4. Indicated by the dashed lines are the conduction and valence band edge energies in the bulk of the device far away from the tip. The plots are (a) for +3 V and (b) for −3 V voltage applied to the sample.

At this stage we address the physical origin of this potential distribution. First we concentrate on negative values applied to the sample. The tip induces a downward band bending for all tip locations relative to the interface. The magnitude of the band bending is a function of the screening by free charge carriers and charged acceptors or donors. In *n*-doped material the downward band bending pushes the conduction band edge below the Fermi energy for negative voltages. Thus, the conduction band bottom on the *n*-doped side is populated by electrons in high concentrations (accumulation) due to the high density of conduction band states. These free electrons screen very effectively the field penetrating into the semiconductor, such that the energetic position of the conduction band edge remains essentially unchanged. This effect occurs in the depletion zone too, until the potential change within the *p*-*n* junction increased enough to shift the conduction band edge above the Fermi energy. Only then the surface potential changes, because no electrons screen anymore. This happens directly at the electronic interface. In the *p*-doped region the tip repels the free holes and only negatively charged acceptors can screen the field of the tip. Within the depletion zone the acceptors are already charged due to the build in potential of the *p*-*n* junction and thus the field of the tip causes additional band bending. As the concentration of acceptors is relatively small in comparison to the density of states in the bands the additional band bending by the tip is significant. Both effects together, the screening by accumulated electrons in the *n*-doped layer and screening by acceptors in the *p*-doped layer, lead to the change of the surface potential only within the *p*-doped region. When moving the tip from the interface into the *p*-doped region, the surface potential changes thus up to the edge of the depletion zone to reach a constant value in the normal *p*-type region [Fig. 5(b)].

At positive voltages the effects are only reversed, with free holes screening in the *p*-type region and positively charged donors in the *n*-type region. This leads to a change of the surface potential only within the *n*-doped region from the interface up to the edge of the depletion zone [Fig. 5(a)].

### D. Tunneling current

The tunneling current between the tip and the semiconductor is determined by the energetic positions of the band edges underneath the tip. The contrast in the STM image reflects thus the surface potential of the *p*-*n*-junction–STM-tip system via the tunneling current. In the following we discuss the tunnel current in this system. The tunnel current is composed of two contributions. (i) Tunneling out of filled valence or into empty conduction band states for negative and positive voltages, respectively. (ii) Tunneling out of or into accumulation layers at the surface for negative and positive voltages, respectively. First we discuss contribution (i) to the tunnel current.

At positive voltages [Fig. 5(a)] the number of empty conduction band states, in which electrons can tunnel from the tip increases when moving the tip from the *p*-doped to the *n*-doped area. Thus one should expect the current to increase monotonically and the increase is spatially localized between the interface and the edge of the depletion zone on the *n*-doped side of the junction. This is in agreement with the observation (see height profiles in Fig. 3). For higher positive voltage the relative difference in the number of conduction band states available for tunneling on the *n*- and *p*-doped sides of the junction decreases. This explains the decrease in contrast found experimentally with increasing voltage.

At negative tunneling voltage an analogous situation occurs. The number of filled valence band states increases from the *n*-doped to the *p*-doped side. Thus one should expect a monotonic increase of the tunnel current when moving the tip from the *n*-doped into the *p*-doped layer. The increase should be localized between the interface and the edge of the depletion zone on the *p*-doped side of the junction. This is observed only for high magnitudes of negative voltages.

However, at smaller magnitudes of negative voltages a pronounced depression occurs. If the current was solely based on valence band states this behavior would imply that the valence band would have to be strongly bend downward near the interface to values below those found on the *n*-doped side of the junction. The bands, however, cannot bend down significantly further, because on *n*-type GaAs the field of the tip is screened even for small negative voltages by a high density of free electrons in the conduction band as mentioned above. Thus the depression cannot be explained solely on basis of the band bending.

In addition, the shift of the registry of the corrugation maxima observed at small negative voltages, where the depression line appears [Fig. 1(b)] indicates that different sublattices are imaged on the *n*- and *p*-doped side. The corrugation maxima correspond to the location of arsenic derived states, if the dominating states involved in the tunneling are energetically in the valence band, and to the location of gallium derived states in case the dominating states are in the conduction band.[22–24] The shift in registry of Fig. 1(b) indicates, that the states involved in the tunneling are different on the *p*- and *n*-type side. Thus we need to discuss the second contribution to the tunnel current mentioned above under (ii).

For negative voltage the electrons can also tunnel from filled conduction band states (accumulation layer) into empty tip states. The existence of such a component in the tunneling current has been shown previously in scanning tunneling microscopy and spectroscopy.[16,23] As already mentioned and seen in Fig. 5(b), the tip-induced band bending is strong enough in the *n*-doped region to establish the accumulation needed for tunneling out of conduction band states. In the *p*-doped region, however, no electrons in the conduction band exist, because the bands are not bent downward enough.

We can now describe the tunneling process across a *p*-*n* junction as follows for negative voltage: While the tip is above the *n*-type material, tip-induced band bending causes an electron accumulation at the surface underneath the tip. As a result the tunneling current is composed of electrons tunneling out of valence and conduction band states in the *n*-type layer. Once the tip is close to the interface, the build-in potential of the junction lifts the conduction and valence band edge upward. Thereby the current component originating from filled conduction band states is ‘‘cut off.’’ Only the component from the valence band contributes now to the tunneling current. When moving the tip towards the *p*-type area, the number of the valence band states is increasing causing the current to increase. The total current change and the decrease of the tip-sample separation near the interface is thus governed by the relative strength of the two components. The higher the negative bias is the more the valence band states contribute and the effect of the ‘‘cut off’’ component is diminished, yielding the more monotonic change in contrast found at higher negative bias, which is limited to the *p*-doped side of the junction.

A similar effect should occur for positive sample voltages too. However, the component to the tunnel current based on tunneling into empty valence band states is about three orders of magnitude smaller than the current tunneling into the conduction band states, because of the much larger barrier. Therefore, we cannot observe a depression at positive voltages.

In this context one can also explain the observed shift in the position of the corrugation maxima seen at low negative voltages [Fig. 1(a)]. On the $n$-type side the tunneling current is composed of electrons tunneling out of valence and conduction band states. At low voltages the corrugation maxima correspond to filled Ga derived surface states energetically located in the conduction band.[23] At the electronic interface the conduction band edge is pulled above the Fermi level and the conduction band component in the current is cut off, leaving only current from the valence band at the interface and in the $p$-type layer. Thus the maxima in the images display arsenic derived surface states that are energetically located in the valence band. On the (110) surface the positions of the arsenic atoms are shifted half a unit cell along the $[1\bar{1}0]$ direction in respect to the gallium atoms which is corresponding to the shift observed.

### E. Extraction of interface properties

On the above background it is obvious that the extraction of physical values of $p$-$n$ junction from STM images is severely affected by the tip. Nevertheless one can provide a method to extract accurately (i) the width of the depletion zone, (ii) the position of the electronic interface, and (iii) the position of the metallurgical interface.

(i) In order to determine the total width of the depletion zone of $p$-$n$ junctions from STM images, one must add the lateral extensions of the monotonic height changes in profiles observed on the $p$-doped side at large negative voltages and on the $n$-doped side at positive voltages. In our case we extract from Fig. 3 values of about 15 nm on the $p$-doped as well as $n$-doped side. Thus the experimentally extracted depletion width is about 30 nm. This is in good agreement with the calculated depletion width (Fig. 5 dashed lines).

(ii) The experimental data shows that the position of the depression line corresponds to the electronic interface, i.e., the plane where the Fermi energy is at midgap. At this position no contribution to the tunnel current exists from filled conduction band states and the increase of the current from the valence band states due to the changing surface potential is only starting. Both together minimize the current, leading to the depression line. Thus the depression line is within a few lattice constants at the position of the electronic interface.

(iii) The metallurgical interface may well be different from the electronic interface for asymmetric doping concentrations[8,9] and/or due to the screening around individual dopant atoms near the interface as well as the clustering of dopant atoms as shown in Ref. 11. The position of the metallurgical interface can only be obtained from the direct observation of the position of the individual dopant atoms in STM images.

## V. CONCLUSION

Combined voltage-dependent atomically resolved scanning tunneling microscopy images, local scanning tunneling spectroscopy, and simulations of the potential distribution in the interface-STM tip system are used to extract the physical imaging mechanisms of GaAs $p$-$n$ junctions in STM images. The voltage-dependent contrast of the $p$-$n$ junction in STM images is found to originate from the build-in potential of the $p$-$n$ junction, which is, however, strongly modulated by the tip-induced band bending, which changes the potential near the interface. As a result at the interface the tunneling characteristics of $p$-type ($n$-type) material are dragged into the interfaces' depletion region at positive (negative) sample voltage. Consequently, the transition region in the STM image does not coincide with the true depletion region and the apparent width of the image of the depletion zone in STM images is reduced considerably compared to the width of the depletion zone in the bulk. Furthermore, at small magnitudes of negative sample voltages, a pronounced depression line appears. The depression is directly correlated with the electronic interface and not with the metallurgical interface. It arises from the interplay of competing current contributions originating from the valence and conduction bands.

On basis of this physical understanding of the imaging process, we developed methods on how to extract accurately physical data about the interfaces' properties from scanning tunneling microscopy images: (i) The spatial location of the electronic interface itself, i.e., the plane where the Fermi energy crosses the midgap position, can be extracted at small magnitudes of negative voltages from the position of the depression line in constant-current STM images. (ii) The *real bulk* width of the depletion zone can be extracted accurately from voltage-dependent STM images. It is the sum of the distances between the interface and the location, where the tip-height remains constant, measured from the interface toward the $n$-doped side at positive voltages and from the interface toward the $p$-doped side at negative tunneling voltages. (iii) The metallurgical interface can be only identified by the positions of the individual dopant atoms imaged in STM images.

*Note added in proof.* Figures 1 and 2 show that at negative voltages the $p$-type layer appears brighter than the $n$-type layer. However, we also observe under identical tunneling conditions that the $n$-type layer is brighter than the $p$-type layer and we occasionally find contrast reversals (connected with tip changes) within a single image. This shows that the absolute contrast level between $p$- and $n$-doped layers is also tip dependent. In fact changes of the tip state were found to induce changes in the relative current contributions extracted from the valence band states and from the accumulation layer (in the conduction band).[25] In our case this means that a brighter contrast of the $n$-type layer at negative voltages arises from an increased current out of the tip-induced accumulation layer in the conduction band states. This effect does not affect any of the explanations and conclusions presented above.

## ACKNOWLEDGMENTS

The authors thank W. K. Liu from IQE Inc. for providing the sample and the Deutsche Forschungsgemeinschaft under Grant No. Eb 197/2-1 as well as the Director, Office of Energy Research, Office of Basic Energy Research, Materials Science Division, U.S. Department of Energy under Contract No. DE-AC03-76SF00098 for financial support.

*Corresponding author. Email address: p.ebert@fz-juelich.de

[1] R. M. Feenstra, Semicond. Sci. Technol. **9**, 2157 (1994); E. T. Yu, Chem. Rev. **97**, 1017 (1997); N. D. Jäger, E. R. Weber, and M. Salmeron, in *Microprobe Characterization of Optoelectronic Materials*, edited by J. Jiménez (Taylor & Francis, London, 2002), p. 303.

[2] E. T. Yu, M. B. Johnson, and J. M. Halbout, Appl. Phys. Lett. **61**, 201 (1992).

[3] M. L. Hildner, R. J. Phaneuf, and E. D. Williams, Appl. Phys. Lett. **72**, 3314 (1998).

[4] R. Chapman, M. Kellam, S. Goodwin-Johansson, J. Russ, G. E. McGuire, and K. Kjoller, J. Vac. Sci. Technol. B **10**, 502 (1992).

[5] W. F. Tseng, J. A. Dagata, R. M. Silver, J. Fu, and J. R. Lowney, J. Vac. Sci. Technol. B **12**, 373 (1994).

[6] A. R. Smith, S. Gwo, K. Sadra, Y. C. Shih, B. G. Streetman, and C. K. Shih, J. Vac. Sci. Technol. B **12**, 2610 (1994).

[7] S. Gwo, A. R. Smith, C. K. Shih, K. Sadra, and B. G. Streetman, Appl. Phys. Lett. **61**, 1104 (1992).

[8] R. M. Feenstra, E. T. Yu, J. M. Woodall, P. D. Kirchner, C. L. Lin, and G. D. Pettit, Appl. Phys. Lett. **61**, 795 (1992).

[9] R. M. Feenstra, A. Vaterlaus, E. T. Yu, P. D. Kirchner, C. L. Lin, J. M. Woodall, and G. D. Pettit, in *Semiconductor Interfaces at the Sub-Nanometer Scale*, edited by H. W. M. Salemink and M. D. Pashley (Kluwer Academic, Dordrecht, 1993), p. 127.

[10] Y. Dong, R. M. Feenstra, R. Hey, and K. H. Ploog, J. Vac. Sci. Technol. B **20**, 1677 (2002).

[11] N. D. Jäger, K. Urban, E. R. Weber, and Ph. Ebert, Phys. Rev. B **65**, 235302 (2002).

[12] H. Edwards, R. McGlothlin, R. San Martin, E. U. M. Gribelyuk, R. Mahaffy, C. K. Shih, R. S. List, and V. A. Ukraintsev, Appl. Phys. Lett. **72**, 698 (1998).

[13] M. L. O'Malley, G. L. Timp, S. V. Moccio, J. P. Garno, and R. N. Kleiman, Appl. Phys. Lett. **74**, 272 (1999).

[14] Ph. Ebert, Surf. Sci. Rep. **33**, 121 (1999).

[15] N. D. Jäger, Ph. Ebert, K. Urban, R. Krause-Rehberg, and E. R. Weber, Phys. Rev. B **65**, 195318 (2002).

[16] R. M. Feenstra and J. A. Stroscio, J. Vac. Sci. Technol. B **5**, 923 (1987). The current originating from the accumulation layer is also called dopant induced feature.

[17] W. E. Spicer, I. Lindau, P. Skeath, C. Y. Su, and P. Chye, Phys. Rev. Lett. **44**, 420 (1980).

[18] J. Tersoff, Phys. Rev. Lett. **52**, 465 (1984).

[19] S. G. Louie and M. L. Cohen, Phys. Rev. B **13**, 2461 (1976).

[20] M. van Schilfgaarde and N. Newman, Phys. Rev. Lett. **65**, 2728 (1990).

[21] SILVACO International, 4701 Patrick Henry Drive, Bldg. 1, Santa Clara, CA 94054.

[22] R. M. Feenstra, J. A. Stroscio, J. Tersoff, and A. P. Fein, Phys. Rev. Lett. **58**, 1192 (1987).

[23] N. D. Jäger, E. R. Weber, and M. Salmeron, J. Vac. Sci. Technol. B **19**, 511 (2001).

[24] Ph. Ebert, B. Engels, P. Richard, K. Schroeder, S. Blügel, C. Domke, M. Heinrich, and K. Urban, Phys. Rev. Lett. **77**, 2997 (1996).

[25] N. D. Jäger, E. R. Weber, K. Urban, and Ph. Ebert, Phys. Rev B (to be published).